Available online at www.sciencedirect.com
SCIENCE DIRECT
Catalysis Today 114 (2006) 197–204
CATALYSIS TODAY
www.elsevier.com/locate/cattod

Thermal stability and siting of aluminum in isostructural ZSM-22 and Theta-1 zeolites

Miroslaw Derewinski [a], Priit Sarv [b,*], Amparo Mifsud [c]

[a] Institute of Catalysis and Surface Chemistry, Polish Academy of Sciences, Niezapominajek 8, PL-30239 Krakow, Poland
[b] Institute of Chemical Physics and Biophysics, Estonian Academy of Sciences, Akadeemia 23, EE-12618 Tallinn, Estonia
[c] Instituto de Tecnologia Quimica UPV-CSIC, Universidad Politecnica de Valencia, Avenida de los Naranjos, SP-46071 Valencia, Spain

Available online 24 February 2006

Abstract

Conventional ^{29}Si and ^{27}Al MAS NMR techniques and ^{27}Al two-dimensional Multiple Quantum Magic Angle Spinning (2D MQMAS) NMR technique were used to characterize two isostructural TON type zeolites (Theta-1, ZSM-22). Nonuniform distribution of framework aluminum and the preferential population of T3 and T4 sites by the aluminum atoms in the TON material were established. The aluminum sites of Theta-1 sample showed higher thermal stability compared to ZSM-22 sample, despite of the higher aluminum content and higher calcination temperature. It was shown that ^{27}Al 2D MQMAS NMR technique can be used for monitoring the minute differences in the surrounding of aluminum T sites, caused by the different templates and the post-synthesis treatments.

Keywords: ZSM-22; Theta-1; ^{27}Al MAS NMR; ^{29}Si MAS NMR; Al distribution; Dealumination

1. Introduction

The activity and selectivity of zeolite-based catalysts in the catalytic processes strongly depend on aluminum distribution in the zeolitic framework. ^{29}Si and ^{27}Al MAS NMR is widely used to study the as made, but also treated zeolite materials, to determine the location and chemical surrounding of silicon and aluminum atoms. Whereas ^{29}Si MAS NMR shows the distribution of silicon tetrahedral sites, the main information one can get from ^{27}Al MAS NMR is the distribution of aluminum between the framework and nonframework sites [1]. A two-dimensional multiple quantum MAS NMR (2D MQMAS NMR) technique provides higher resolution than the conventional one-dimensional techniques, enabling one to detect several nonequivalent tetrahedral aluminum sites [2–4]. Therefore, there exist means to study the effect of post synthesis treatments directly on the aluminum tetrahedral sites [5,6]. In the present study we used the 2D MQMAS NMR to determine the aluminum distribution in the TON type zeolites (Theta-1 and ZSM-22) and monitor the effect of post-synthesis treatments.

2. Experimental

Two isostructural TON type zeolites (Theta-1 and ZSM-22) with different Si/Al ratio (39 for Theta-1 and 77 for ZSM-22) were synthesized hydrothermally at 160 °C. The synthesis of ZSM-22 was carried out using 1-ethyl pyridinium bromide (EtPBr) as template following the procedure reported in reference [7]. Sodium silicate (Merck, extra pure), laboratory made EtPBr, sulfuric acid (POCh, pure), aluminum sulfate (POCh, analytical grade) and doubly distillated water were used for the synthesis of ZSM-22. The molar composition of the gel used for the synthesis was: $(EtPBr)_{35}$ $(Na_2O)_{105}$ $(Al_2O_3)_1$ $(SiO_2)_{185}$ $(H_2O)_{8900}$. The prepared mixture was aged for 20 h at room temperature and subsequently the synthesis was carried out in the static conditions for 4 days.

Theta-1 zeolite was synthesized in stirring conditions using diethanolamine (DEA) as template, following the procedure described in reference [8]. For this synthesis colloidal silica Ludox AS40 (Aldrich, pure), sodium aluminate (Carlo Erba RLE), sodium hydroxide (POCh, analytical grade), diethanolamine (POCh, analytical grade) and doubly distillated water were used. The molar composition of the gel was: $(DEA)_{38}$ $(Na_2O)_6$ $(Al_2O_3)_1$ $(SiO_2)_{55}$ $(H_2O)_{1100}$. The prepared gel was aged for 15 h while stirring prior to the crystallization, then

* Corresponding author.

0920-5861/$ – see front matter © 2006 Elsevier B.V. All rights reserved.
doi:10.1016/j.cattod.2006.01.008

transferred to Teflon-lined autoclaves and heated at 160 °C for 55 h.

After crystallization the solids were filtered, washed up to pH 9 with de-ionized water and dried at 90 °C overnight. The as-made materials were calcined (ZSM-22 at 520 °C and Theta-1 at 600 °C) in dry air (80 cm^3/min) and subsequently ion-exchanged with 1 M NH_4NO_3 solution at 60 °C for 24 h.

The samples were characterized with XRD, SEM and ^{27}Al MAS NMR spectroscopy. The XRD patterns were measured on Siemens 5005 spectrometer using Cu Kα radiation. The SEM pictures were taken with a Philips XL30 instrument. The MAS NMR spectra were taken on a Bruker AMX500 spectrometer using a custom-built (3.5 mm o.d. rotor) probehead. The spinning speed was approximately 15 kHz. ^{29}Si MAS NMR spectra were taken with a 30° pulse, a relaxation delay of 8 s and 2000 scans were accumulated. For MQMAS experiments the AMX500 was equipped with additional 250 W power amplifier to ensure the radio-frequency (rf) field strength of 120 kHz. $KAl(SO_4)_2{\cdot}12H_2O$ was used as an external reference for quantitative ^{27}Al experiments and as a chemical shift reference ($^{27Al}\delta_{CS} = 0$ relative to 1 M solution of $Al(NO_3)_3$). 1D single pulse ^{27}Al MAS NMR experiments had the following parameters: flip angle of the exciting pulse was about 10°; relaxation delay was 0.2 s and 20,000 scans were accumulated. All 1D spectra were analyzed with a Bruker 1D WIN NMR software. Prior to the NMR measurements the samples were kept at 75% relative humidity for at least 48 h.

Since we anticipated the distribution of quadrupolar coupling constants, we started with the ^{27}Al 3Q MAS NMR experiments instead of 5Q experiments. Three quantum transitions have a wider excitation profile with respect to quadrupolar interaction [9]. In a second stage the ^{27}Al 5Q MAS NMR experiments were performed to increase the resolution, but we could not retrieve any additional aluminum sites to those already seen in the 3Q spectra. The 3Q MAS NMR experiments were performed with a three-pulse sequence using symmetrical coherence transfer pathways $-0 > (\pm 3) > 0 > (-1)$ [10]. Longer relaxation delays of 0.4 s were used, since higher order transitions tend to have longer relaxation times compared to the central transition [11]. Rotation speed was reduced to 11 kHz in order to get better excitation of multiple quantum coherences and rotation synchronized data acquisition in t_1 dimension was used to reduce the signal acquisition time and avoid the folding of the spinning sidebands [12]. The first pulse had the duration of 3.2 μs, the second pulse was 1.2 μs and the third pulse was 7.9 μs. The rf strength of the third pulse was reduced to approximately 10 kHz. All three pulses were optimized prior to the 2D experiment for the maximum signal intensity. 2D NMR signal was acquired (1200 scans) with the States-TPPI method and a shearing transformation was performed by employing a t_1 dependent first order phase correction in the mixed (t_1, ν_2)-domain, after constructing echo and antiecho signals [13].

3. Results and discussion

The X-ray diffraction (XRD) is used to prove that the product we have got after synthesis is TON type zeolite. Then we present the scanning electron microscopy (SEM) data to show the crystal morphology of the materials under study. It has relevance to the dealumination process during calcination, which was studied with the quantitative ^{27}Al MAS NMR. The ^{27}Al 2D MQMAS NMR and ^{29}Si MAS NMR data of the present paper plus previously published XRD data [19] were used to study the siting of aluminum in the framework. Finally, we demonstrate how the information gained from the high-resolution isotropic projections of the ^{27}Al 2D MQMAS NMR spectra sheds light into the subtle differences of ZSM-22 and Theta-1 samples during calcination and ion-exchange.

3.1. XRD

The X-ray diffraction patterns of as-synthesized ZSM-22 and Theta-1 are in good agreement with the data published for the TON type zeolites [14]. XRD analysis has shown that both samples are highly crystalline. There is no unreacted, amorphous material (Fig. 1).

3.2. SEM

The results of SEM analysis are given in Fig. 2. ZSM-22 and Theta-1 samples exhibit significantly different morphology and crystal size. ZSM-22 forms rice-like crystals up to 16 μm in length and 5 μm in width, but Theta-1 forms aggregates of very fine (1 × 0.2 μm) randomly oriented crystals. SEM data confirm high crystallinity of ZSM-22 and Theta-1 samples and purity of both preparations.

3.3. NMR

Both as-made materials have all the aluminum in tetrahedral framework positions. The amount of aluminum atoms estimated by chemical analysis (13×10^{16} aluminum atoms/mg and 25×10^{16} atoms/mg for ZSM-22 and Theta-1,

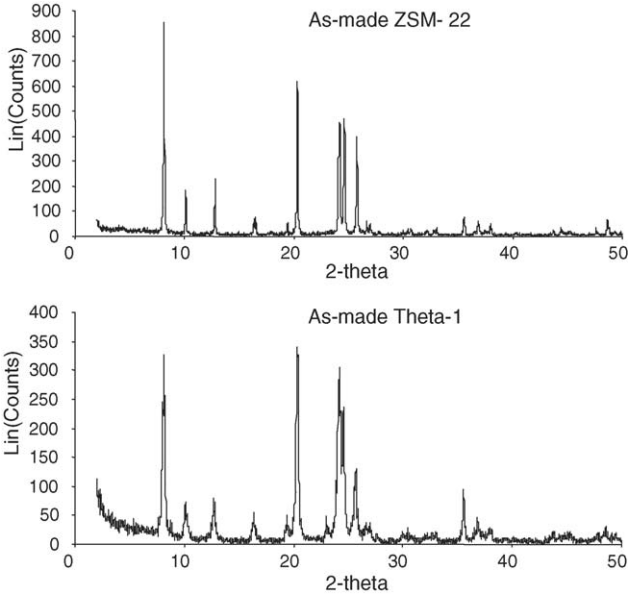

Fig. 1. X-ray diffraction patterns of as-made ZSM-22 and Theta-1.

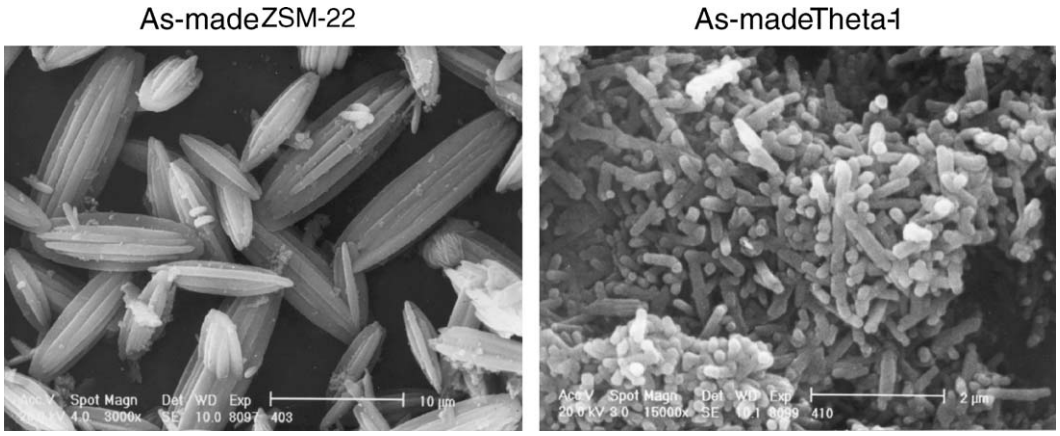

Fig. 2. The SEM pictures of as-made ZSM-22 and Theta-1.

respectively) is comparable to the results got from the ^{27}Al MAS NMR experiments (Table 1: 13×10^{16} aluminum atoms/mg and 28×10^{16} atoms/mg, respectively). Therefore, we may conclude, that we are detecting all the aluminum atoms.

Calcination produces hexacoordinated aluminum sites in both samples. In calcined ZSM-22 about 1/3 of aluminum sites are in six-coordinated environment and in calcined Theta-1 there are only about 10% of aluminum sites in octahedral positions (Table 1, Fig. 3). Quantitative analysis of ^{27}Al NMR spectra (Fig. 3, Table 1) revealed that in ZSM-22 half of the octahedral aluminum, produced after calcination, transformed back to tetrahedral aluminum after ion-exchange. In Theta-1 sample the octahedral aluminum was mostly removed from the material during the ion-exchange process. Different behavior of the two isostructural materials under study could be the result of several factors. The thermal analysis of the samples showed, that the decomposition of strongly bonded bulky 1-ethyl pyridinium cations in ZSM-22 sample takes place at considerably higher temperature, than the decomposition of diethanolamine in Theta-1 sample (maximum temperatures at 450 and 397 °C, respectively). Therefore, we conclude that the preferential dealumination of the ZSM-22 sample compared to Theta-1 is the result of the synergistic effect of higher temperature required for the total oxidation of 1-ethyl pyridinium cations and the crystal size—longer residence time of water and CO_2 molecules in larger crystals of ZSM-22. Moreover, the EtPBr containing more carbon atoms produces significantly more heat during the oxidation of the residual carbon-rich organic species, which can result in overheating of the ZSM-22 sample.

Table 1
Results of the quantitative ^{27}Al MAS NMR experiments

Sample	Tetrahedral (Al/mg $\pm 1 \times 10^{16}$)	Octahedral (Al/mg $\pm 1 \times 10^{16}$)
As-made ZSM-22	13×10^{16}	0
Calcined ZSM-22	8×10^{16}	4×10^{16}
Ion-exchange ZSM-22	13×10^{16}	2×10^{16}
As-made Theta-1	28×10^{16}	0
Calcined Theta-1	26×10^{16}	3×10^{16}
Ion-exchange Theta-1	27×10^{16}	0

The 2D 3Q MAS NMR spectra of the samples under study and their isotropic projections are given in Fig. 4. The 2D spectra of ZSM-22 and Theta-1 samples have considerable differences, reflecting the influence of chemical manipulations on the tetrahedral framework aluminum sites. We use f1 or isotropic projections (vertical axis) of the 2D spectra to extract information about the distribution and chemical shifts of the nonequivalent aluminum sites. The isotropic projections are deconvoluted with gaussian lines to reveal the relative population of different sites. Approximate linewidths and line positions, used in the simulations, are measured from the 2D spectra. The quadrupolar induced shift of the isotropic projection (Qis') is calculated using formulas in reference [6]. The f1 coordinate of the site is obtained from the simulation of the f1 projection and the f2 coordinate is the center of gravity of the respective f1 slice in the 2D spectrum. To get the isotropic chemical shift one has to subtract the Qis' from the line position in f1 dimension, since contrary to the f2 dimension, in the f1 dimension the quadrupolar shift is positive. Generally speaking, the multiple quantum coherences of aluminum atoms with different strength of quadrupolar interaction are excited and detected to different extent [15]. The detection profile depends on the ratio of rf strength and the strength of the quadrupolar interaction. In our samples the quadrupolar interaction never exceeded 2.5 MHz, the rf excitation was 120 kHz and we may consider the relative line intensities as true relative aluminum site intensities (see Fig. 3 in ref. [15]). Therefore in the analysis of the isotropic projections of the MQMAS NMR spectra we have to concentrate ourselves on three parameters—line-position, quadrupolar induced shift and relative intensity (see Fig. 4).

For both zeolites, ZSM-22 and Theta-1, the isotropic projections of ^{27}Al 3Q MAS NMR spectra follow the general trend that the best resolution is achieved for the ion-exchanged samples, where clearly at least two lines, with an approximate ratio 2:3, can be identified. The highly siliceous form of ZSM-22 is known to have four nonequivalent tetrahedral sites with the ratio of 2:1:1:2 and ^{29}Si chemical shifts of −110.8, −112.7, −113.0, and −114.3 ppm, respectively [14]. In the aluminum containing zeolites some of the tetrahedral framework positions are occupied by aluminum and the previously well-resolved

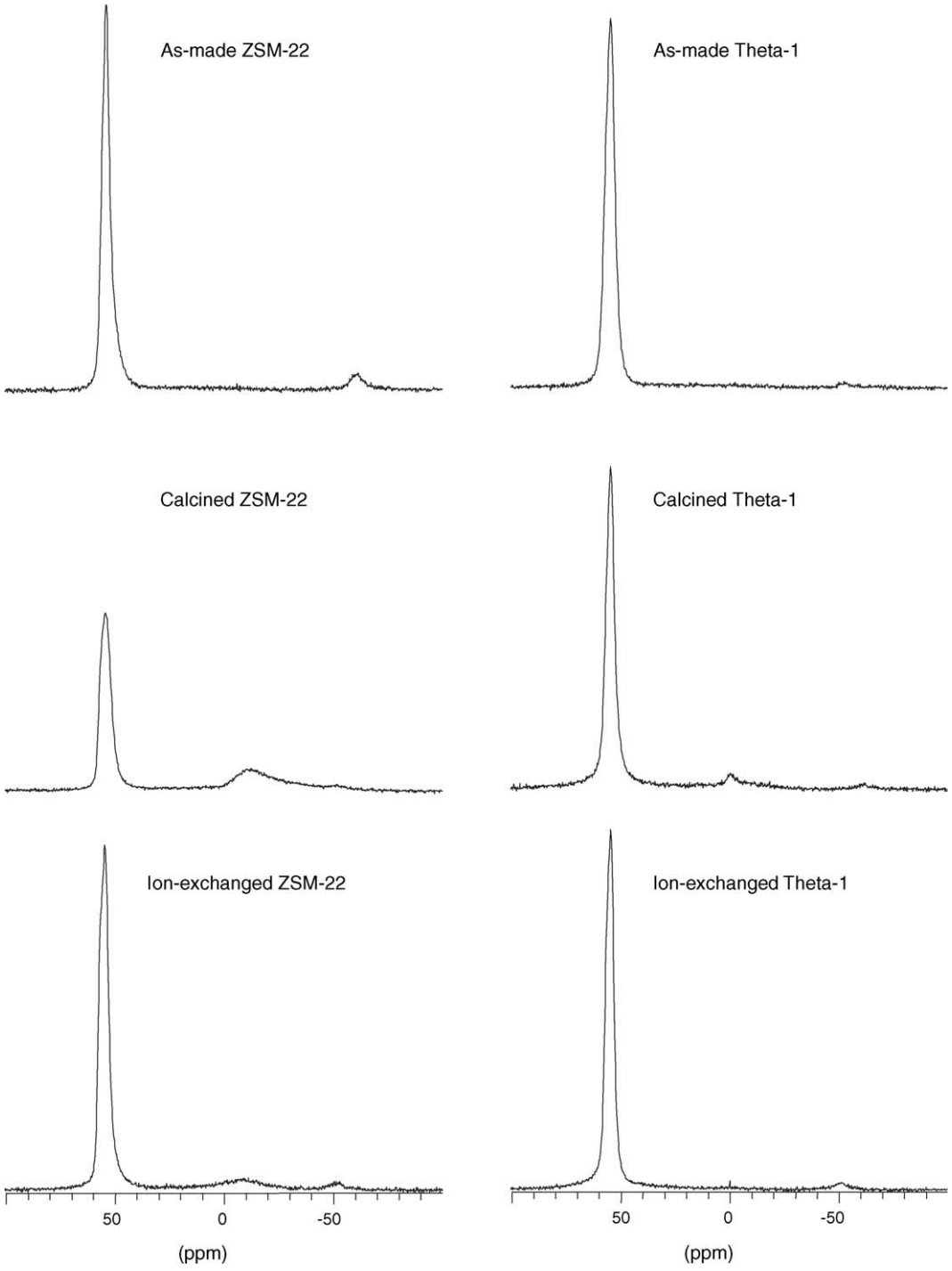

Fig. 3. The ^{27}Al MAS NMR spectra of ZSM-22 and Theta-1 samples. The line-intensities of the same type of zeolite are scaled to equal sample mass. The line at 55 ppm corresponds to four-coordinated aluminum, the line at −10 ppm corresponds to six-coordinated aluminum and the line at −50 ppm corresponds to spinning sideband. Experimental conditions are given in the text.

^{29}Si NMR spectrum becomes broadened. The broadening is caused by the distortions of the T–O–T bond angles induced to accommodate the bigger aluminum tetrahedra and other defect sites (for example silanol nests). It is unclear how far these distortions extend around aluminum site. From the NMR spectra one can see that all aluminum sites and all silicon sites are affected i.e. broadened (Figs. 4 and 5, respectively). Assuming that nonequivalent framework tetrahedral (T) sites are exchanged to the same extent, we expect to see three major lines of the same intensity and width in the −110 to −115 ppm region, corresponding to the −110.8, −112.7/−113.0 and −114.3 ppm lines, respectively. These are the lines corresponding to the Si(4Si) sites from which intensity was drawn to the broad −103 ppm (ZSM-22) and −105 ppm (Theta-1) lines, corresponding to the Si(1Al,3Si) and Si(OH) sites, due to the aluminum insertion during synthesis. Uniform replacement

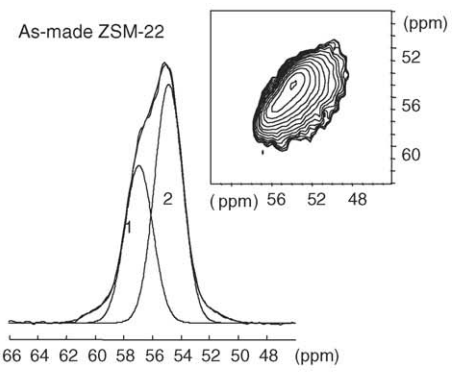

No.	Pos.(ppm)	Width(ppm)	Int.(rel.)	Qis(ppm)
1	56.9	2.3	40	0.6
2	54.9	2.3	60	0.4

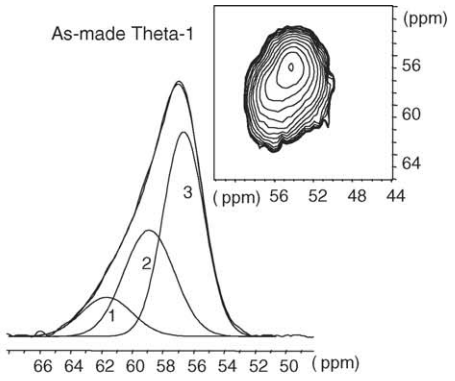

No.	Pos.(ppm)	Width(ppm)	Int.(rel.)	Qis(ppm)
1	61.6	3.3	13	2.3
2	58.9	3.3	34	1.1
3	56.6	2.7	53	0.9

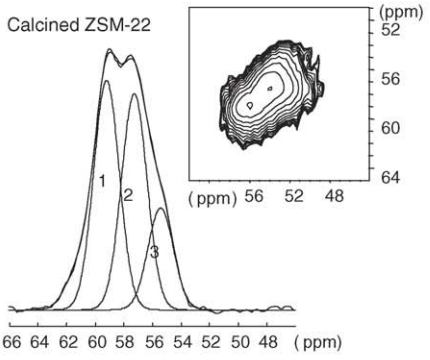

No.	Pos.(ppm)	Width(ppm)	Int.(rel.)	Qis(ppm)
1	59.2	2.1	45	1.2
2	57.3	2.1	37	1.3
3	55.5	2.1	17	0.9

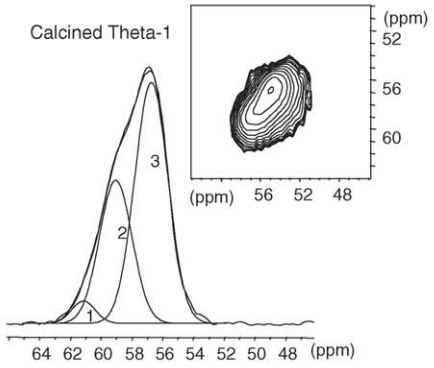

No.	Pos.(ppm)	Width(ppm)	Int.(rel.)	Qis(ppm)
1	61.1	1.5	4	1.5
2	59.0	2.1	35	0.7
3	56.7	2.2	61	0.7

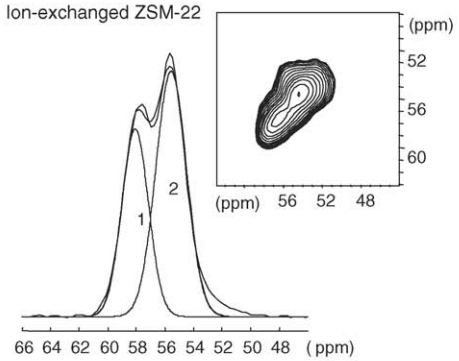

No.	Pos.(ppm)	Width(ppm)	Int.(rel.)	Qis(ppm)
1	58.1	2.2	40	0.5
2	55.6	2.5	60	0.5

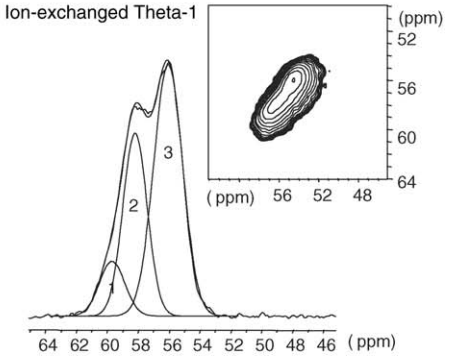

No.	Pos.(ppm)	Width(ppm)	Int.(rel.)	Qis(ppm)
1	59.7	1.6	11	1.0
2	58.2	1.6	34	0.6
3	56.1	1.9	56	0.6

Fig. 4. Isotropic projections of the 2D 3QMAS NMR spectra of ZSM-22 and Theta-1 samples together with deconvolutions and deconvolution parameters. The inserts show the respective 2D 3QMAS NMR spectra from which the projections were taken. Experimental conditions are given in the text.

should leave the lines at −114.5, −112.5 and −111 ppm with the same width and intensity. However, one can see that this is not the case: −112.5 ppm line has higher intensity, meaning that these sites were less affected by the aluminum insertion. In the case of ZSM-22 sample the line-intensity differences are quite small due to smaller aluminum concentration, but in the case of Theta-1 they are distinct. As was mentioned before, also aluminum NMR spectra cannot be simulated using three lines of the same width and intensity (Fig. 4). So, a general conclusion is that aluminum is not uniformly distributed over the possible nonequivalent framework T sites in our Theta-1 and ZSM-22 samples. Our previous studies of other 10-membered ring zeolites, MFI and FER, with similar Si/Al = 50 ratio, have shown that aluminum is uniformly distributed between nonequivalent framework T sites ([5,6]). On the other hand, paper by Han et al. claims the existence of nonuniform distribution of aluminum in ZSM-5 [16]. We believe the discrepancy is caused by considerably lower Si/Al ratio of the ZSM-5 samples they studied.

To find out which tetrahedral silicon site corresponds to which tetrahedral aluminum site, one has to compare the average T–O–T angles calculated for both sites using the known empirical formulas. For the Al T–O–T bond angle we used the equation $^{Al}\delta = -0.500 \times \bar{\alpha} + 132$ [17] and for Si we used the relation $^{Si}\delta = -0.5793 \times \bar{\alpha} - 25.44$ [18]. We note that these two empirical equations correlate the NMR data with the X-ray data, which in the case of aluminosilicate zeolites in general cannot distinguish between Al and Si tetrahedral sites. Therefore, the ambiguous notation T–O–T is used, instead of Al–O–Si or Si–O–Si. In Table 2 we gathered the T–O–T angles calculated from the data of four different sources: ^{29}Si chemical shifts of the highly siliceous ZSM-22 [14] and of the TON type

Table 2
Comparison of average T–O–T angles of tetrahedral sites in TON type zeolites

Sample	Line no. in Fig. 4[e]	$^{27Al}\delta$ (ppm)	⟨T–O–T⟩ (°)[f]	Relative population of the site (%)	Tetrahedral position[c]
As-made silica ZSM-22[a]			148	33	T1
			151	17	T3
			152	17	T4
			153	33	T2
Silica ZSM-22[b]			147	33	T1
			151	17	T3
			151	17	T4
			153	33	T2
Ion-exchange ZSM-22[d]			148 ± 2		T1
			150 ± 2		T3 + T4
			153 ± 2		T2
Ion-exchange Theta-1[d]			148 ± 2		T1
			151 ± 2		T3 + T4
			154 ± 2		T2
As-made ZSM-22[e]	1	56.3	151 ± 2	40	
	2	54.5	155 ± 2	60	
Calcined ZSM-22[e]	1	58.0	148 ± 2	45	T1 + T3 + T4
	2	56.0	152 ± 2	37	T2 + T3 + T4
	3	54.6	155 ± 2	18	T2
Ion-exchange ZSM-22[e]	1	57.6	149 ± 2	40	T1 + T3 + T4
	2	55.1	154 ± 3	60	T2 + T3 + T4
As-made Theta-1[e]	1	59.3	145 ± 5	13	T1
	2	57.8	148 ± 2	34	T1 + T3 + T4
	3	55.7	153 ± 3	53	T2 + T3 + T4
Calcined Theta-1[e]	1	59.6	145 ± 3	4	T1
	2	58.3	147 ± 2	35	T1 + T3 + T4
	3	56.0	152 ± 2	61	T2 + T3 + T4
Ion-exchange Theta-1[e]	1	58.7	147 ± 2	11	T1
	2	57.6	149 ± 2	34	T1 + T3 + T4
	3	55.5	153 ± 2	56	T2 + T3 + T4

[a] Average T–O–T angles are calculated from the Si–O–Si angles given in reference [19].
[b] Average T–O–T angles are calculated from the ^{29}Si chemical shifts given in ref. [14] and using relation in reference [18].
[c] Assignments to T-sites based on ⟨T–O–T⟩ angle.
[d] Average Si–O–Si angles were calculated using ^{29}Si chemical shifts from Fig. 5.
[e] Average T–O–T angles were calculated using ^{27}Al isotropic chemical shifts from Fig. 4.
[f] Error estimates are calculated from the linewidths of the lines.

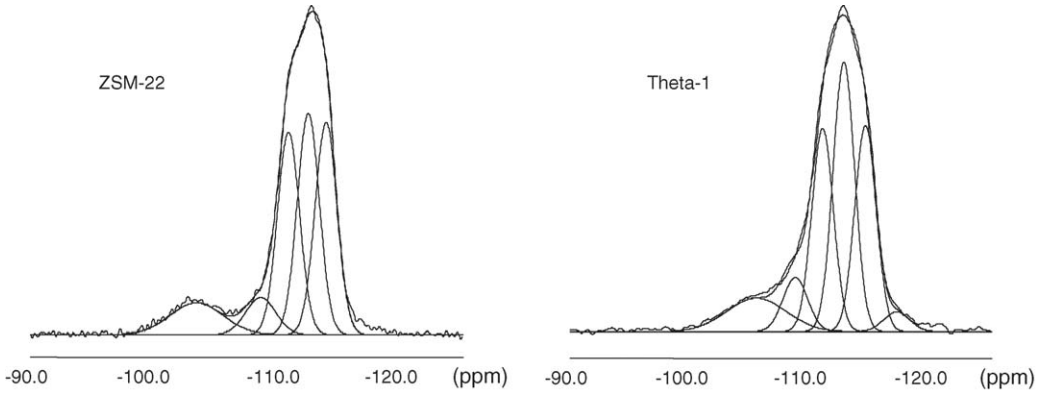

				%
Position	-113.94	Width	2.10	28
Position	-112.49	Width	2.10	29
Position	-110.89	Width	2.10	27
Position	-108.64	Width	2.83	6
Position	-103.46	Width	4.98	10

				%
Position	-117.12	Width	2.56	3
Position	-114.53	Width	2.10	24
Position	-112.74	Width	2.10	31
Position	-110.97	Width	2.10	24
Position	-108.71	Width	2.42	7
Position	-105.48	Width	5.79	11

Fig. 5. ^{29}Si MAS NMR spectra of ion-exchanged ZSM-22 and Theta-1.

zeolites studied in the present paper (Fig. 5); ^{27}Al chemical shifts (Fig. 4) and XRD [19].

The assignment of the aluminum NMR spectrum lines to the T sites (last column of Table 2) is based solely on the average T–O–T angle calculated from the isotropic chemical shift. From Fig. 4 one can see how sensitive the average T–O–T angle, detected by the 2D MQMAS NMR technique, is to subtle differences in the surrounding of the aluminum T sites, caused by the sample treatments: as-made samples of ZSM-22 and Theta-1 having different templates; calcination producing different relative concentrations of six-coordinated aluminum and finally ion-exchange producing quite similar aluminum T site distribution. Comparing the average T–O–T angles of ion-exchanged samples, calculated from ^{29}Si and ^{27}Al chemical shifts, one may conclude that aluminum is mainly located in the T1 and T2 sites (boldface in Table 2). Although the existence of T3 and T4 aluminum sites cannot be ruled out, they are populated by aluminum to a smaller extent than T1 and T2 sites. The framework of as-made Theta-1 is more distorted around the aluminum site than in the case of as-made ZSM-22—the lines are broad and there is considerable distribution of the quadrupolar interaction (see Fig. 4). The ^{27}Al chemical shifts of as-made ZSM-22 are about 0.6–1.5 ppm lower than those of as made Theta-1 material. This diamagnetic shift is caused by the aromatic template molecule (1-ethyl pyridinium bromide) and depends on the distance and orientation of the molecule relative to the alumnium site. Therefore the ^{27}Al chemical shifts of as-made ZSM-22 cannot be used for T–O–T calculation directly, but the shift has to be taken into account. The spectrum of calcined ZSM-22 (Fig. 4) shows distorted surrounding of the aluminum T sites, especially for the site that is more shielded. The line corresponding to T2 + T3 + T4 aluminum sites splits into two lines. The effect is caused by the six-coordinated aluminum distorting the zeolitic framework since it is missing in the Theta-1 sample, where the relative concentration of six-coordinated aluminum is considerably lower (Table 1). One may conclude that the six-coordinated aluminum site, created during calcination, is close to the framework aluminum site. This result supports the reasoning that aluminum sites tend to be relatively close to each other, so that the distortions caused by the aluminum tetrahedra may cancel each other and overall energy change of the lattice is minimal [20]. It also means that aluminum is mainly extracted from these paired aluminum sites.

4. Conclusions

ZSM-22 and Theta-1 zeolites were synthesized with 1-ethylpyridinium bromide and diethanolamine, respectively. Samples were characterized with XRD and SEM to check the crystal structure and morphology. The aluminum distribution in as-made and treated zeolites was studied by ^{27}Al 1D MAS NMR and 2D MQMAS NMR. In ZSM-22 and Theta-1 there are nonrandom populations of aluminum between available framework tetrahedral sites. The ^{27}Al 2D MQMAS NMR spectrum gives at least two lines with the relative intensity of 2:3. Based on average T–O–T angles, calculated from the isotropic chemical shifts, we assigned these lines mainly to aluminum atoms in T1 and T2 sites, respectively. T3 and T4 sites are occupied to a smaller extent and they contribute to the overall intensity of the lines, but remain unresolved in the aluminum spectrum. During calcination 1/3 of the aluminum tetrahedral sites in ZSM-22 sample are converted to six-coordinated sites, which are partly transformed back to four-coordinated aluminum after ion-exchange. In spite of the higher Al content the Theta-1 zeolite is more stable during calcination compared to ZSM-22. This is explained by the synergistic effect of large crystals of the ZSM-22 and the template with

more carbon atoms producing significantly more heat during calcination. We showed that minute differences in the surrounding of the framework aluminum T site, caused by templates and extraframework six-coordinated aluminum, can be monitored with the MQMAS NMR technique. In ZSM-22 aluminum sites are possibly located close to each other, since octahedral aluminum sites, produced after calcination, distort the T–O–T angles of framework aluminum sites.

Acknowledgments

Support of this work within the framework of the Polish-Estonian interacademic exchange agreement is gratefully acknowledged. Also, financial support of the work by the Estonian Science Foundation through grant No. 5936 is acknowledged.

References

[1] G. Engelhardt, D. Michel, High-Resolution Solid-State NMR of Silicates and Zeolites, John Wiley & Sons, Chichester, 1987.
[2] L. Frydman, J.S. Harwood, J. Am. Chem. Soc. 117 (1995) 5367.
[3] C. Fernandez, J.P. Amoureux, Chem. Phys. Lett. 242 (1995) 449.
[4] A. Medek, J.S. Harwood, L. Frydman, J. Am. Chem. Soc. 117 (1995) 12779.
[5] P. Sarv, C. Fernandez, J.P. Amoureux, K. Keskinen, J. Phys. Chem. 100 (1996) 19223.
[6] P. Sarv, B. Wichterlová, J. Cejka, J. Phys. Chem. B 102 (1998) 1372.
[7] R. Kumar, P. Ratnasamy, J. Catal. 116 (1989) 440.
[8] F.D. Renzo, F. Remoue, P. Massiani, F. Fajula, F. Figueras, Zeolites 11 (1991) 539.
[9] C. Fernandez, J.P. Amoureux, J.M. Chezeau, L. Delmotte, H. Kessler, Micropor. Mesopor. Mater. 6 (1996) 331.
[10] J.P. Amoureux, C. Fernandez, S. Steuernagel, J. Magn. Reson. A 123 (1996) 116.
[11] E.R. Andrew, D.P. Tunstall, Proc. Phys. Soc. 78 (1961) 1.
[12] D. Massiot, J. Magn. Reson. A 122 (1996) 240.
[13] D. Massiot, B. Touzo, D. Trumeau, J.P. Coutures, J. Virlet, P. Florian, P. Grandinetti, Solid State NMR 6 (1996) 73.
[14] C.A. Fyfe, G.T. Kokotailo, H. Strobl, C.S. Pasztor, G. Barlow, S. Bradley, Zeolites 9 (1989) 531.
[15] J.P. Amoureux, C. Fernandez, L. Frydman, Chem. Phys. Lett. 259 (1996) 347.
[16] O.H. Han, C.S. Kim, S.B. Hong, Angew. Chem. Int. Ed. 41 (2002) 469.
[17] E. Lippmaa, A. Samoson, M. Mägi, J. Am. Chem. Soc. 108 (1986) 1730.
[18] J.M. Thomas, J. Kennedy, S. Ramdas, B.K. Hunter, D.T.B. Tennakoon, Chem. Phys. Lett. 102 (1983) 158.
[19] B. Marler, Zeolites 7 (1987) 393.
[20] K-P. Schröder, J. Sauer, J. Phys. Chem. 97 (1993) 6579.